Computational Fluid Dynamic Simulation with Experimental Validation in Turbine Pipeline

William Oñate, Santiago Maldonado, Sebastián Taco, Gustavo Caiza

Abstract:With the increase of carbon dioxide emissions and greenhouse gases generated by the consumption of fossil fuels, this research considers the use of alternative energy sources, like the tidal energy which stores and contains the water in a reservoir through a dam or levee. This energy is later released and is converted into electrical energy through the unidirectional flushing of the fluid by a turbine pipeline, emerging variables such as pressure, speed magnitude, and turbulent kinetic energy. These variables will be studied using a computer dynamic 2D model simulated by the ANSYS FLUENT software by setting boundary conditions obtained by digital methodology of classical mechanics of fluids. The results were compared with those obtained experimentally through a tidal module, which consists of elements that were selected after criterion arrays, finding that, during the fluid download process for the energy generation, there is a qualitative similarity in the four areas of the pipeline of turbine (entry, final part of the leeward side of the bulb, posterior and anterior to the propeller), as well as the quantitative values presented similarity in two inner points of the turbine pipeline, getting an error of 1.69% and 1.95% respectively, thus validating the prediction.

Index Terms:Alternative energy, bulb, dyke, tidal turbine.

I. INTRODUCTION

The demand for energy is growing around 1.9% per year, proportionally increasing the emissions of CO2 and other greenhouse gases produced by the consumption of more than 80% of fossil fuels, causing environmental pollution and global warming [1]. To reduce these effects, it is proposed to increase the use of clean energy to 21 per cent in the year 2013, and 39% in year 2025 [2].

According to the global energy matrix, the energy of the oceans is the fifth non-conventional renewable energy supply, this is since the ocean occupies the 70% of the land surface containing a large amount of energy [3] - [4].

In Ecuador, the electrical generation by solar, wind and biomass energy are very relevant. However, it is important to be aware of the existence of other alternative energies that, in the future, can be integrated to the national energy matrix, as is the case of tidal energy through the gradient tide (ascent and descent) [5] - [6].

Tidal power plants of the world generate energy of approximately 550 GWh net per year, within which we have: Sihwa Lake in South Korea, The Rance in France, and Annapolis Royal in [7]. This type of power plants has two modes of operation called single effect and double effect. The first one refers to cycles of operation of reflux when the tide drops, and flow when the tide rises [8]. The second mode of operation for the generation occurs in both directions, i.e. in flow and reflow, hence the need for reversible turbines [9]. The parties that make up a tidal central are tidal dam, reservoir, turbine pipeline, gate of water passage and turbine [10]., within which the bulb-type turbine is one of the most important parts, due to the fact that, taking advantage of small jumps with great flow, these turbines are located so that the water moves axially through the contour of the housing with the bulbous guiding water to the dealer, which allows to regulate the flow to let the water to flow with a proper angle for the available power of the system [11].

The paper is organized as follows: Section II describes the concepts, system design and methodology used; Section III shows the analysis of results; and finally, Section IV presents the conclusions.

II. MATERIALS AND METHODS

A. Design

For the preliminary design, a study was made on the tidal module components, using criterion arrays for the selection of the same, such is the case of the reservoir (dimensions under the UNE-EN 13150:2001 standard and characteristics of the material), turbine coefficient pipeline (geometric coefficient) [12]., pressure sensors (accuracy, repeatability, and stability) [13]., a reflective optical sensor (precision), bulb (relative thickness and coefficient of lift [14]., generator (magnetic field, use of brushes, resignations and high speed), propeller (angle of attack, angle of inclination, mass, and diameter [15] - [16].

The process of the tidal equipment for electric power generation begins when the water level in the reservoir is at its maximum level, resulting in the opening of the gate over passing water, obtaining a unidirectional flow of fluid through the pipeline of turbine, thereby achieving the energy generation [17]. Fig. 1 shows the blocks diagram that represents the tidal module.

Revised Manuscript Received on May15, 2019.

William Oñate, Universidad Politécnica Salesiana, GIECA – Electronic, Control and Automation Research Group, Quito, Ecuador.
Santiago Maldonado, Universidad Politécnica Salesiana, Quito, Ecuador.
Sebastían Taco, Escuela Poltécnica Nacional, Quito, Ecuador.
Gustavo Caiza, Universidad Politécnica Salesiana, GIECA – Electronic, Control and Automation Research Group, Quito, Ecuador.

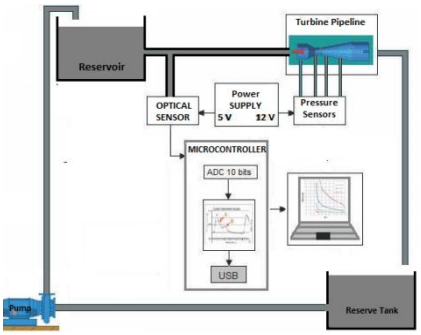

Fig. 1: Block Diagram of the system.

B. Numerical Method Using.

The variables that are in the pipeline for the study are pressure, momentum, turbulent kinetic energy ( ) and the dissipation of energy because of the turbulence ( ), complex mathematics are used for the resolution of nonlinear partial derivatives in the simulation, using a computational package for the Fluid Dynamics in ANSYS FLUENT 17.2 [18]. This software allows to resolve the variables using the Navier Stokes equations. Refer to (1), (2) and (3) [19] - [20].

$$\rho\left\{\frac{\partial V_x}{\partial t}+V_x\frac{\partial V_x}{\partial x}+V_y\frac{\partial V_x}{\partial y}+V_z\frac{\partial V_x}{\partial z}\right\} = \rho f_x-\frac{\partial P}{\partial x}+\mu\left\{\frac{\partial^2 V_x}{\partial x^2}+\frac{\partial^2 V_x}{\partial y^2}+\frac{\partial^2 V_x}{\partial z^2}\right\} \quad (1)$$

$$\rho\left\{\frac{\partial V_y}{\partial t}+V_x\frac{\partial V_y}{\partial x}+V_y\frac{\partial V_y}{\partial y}+V_z\frac{\partial V_y}{\partial z}\right\} = \rho f_y-\frac{\partial P}{\partial y}+\mu\left\{\frac{\partial^2 V_y}{\partial x^2}+\frac{\partial^2 V_y}{\partial y^2}+\frac{\partial^2 V_y}{\partial z^2}\right\} \quad (2)$$

$$\rho\left\{\frac{\partial V_z}{\partial t}+V_x\frac{\partial V_z}{\partial x}+V_y\frac{\partial V_z}{\partial y}+V_z\frac{\partial V_z}{\partial z}\right\} = \rho f_z-\frac{\partial P}{\partial z}+\mu\left\{\frac{\partial^2 V_z}{\partial x^2}+\frac{\partial^2 V_z}{\partial y^2}+\frac{\partial^2 V_z}{\partial z^2}\right\} \quad (3)$$

The boundary conditions of entry and exit of the pipeline of turbine were used for simulation and analysis of the results. These conditions were calculated using the resolution of numerical methods for determining the download of the fluid from the reservoir by the volume control of non-stationary mass [21] - [22]., in addition to the stationary absolute pressures in the four areas of interest inside the turbine duct and the speeds [23]. For this purpose, the researchers employed the principles of classical mechanics of fluids for pipeline, lower and higher load losses, total loss of load on line, drag pressure in hydrodynamic body, drag force of the bulb and drag force [24]. in propeller. Fig. 2 shows the block diagram of the equations used for the boundary conditions.

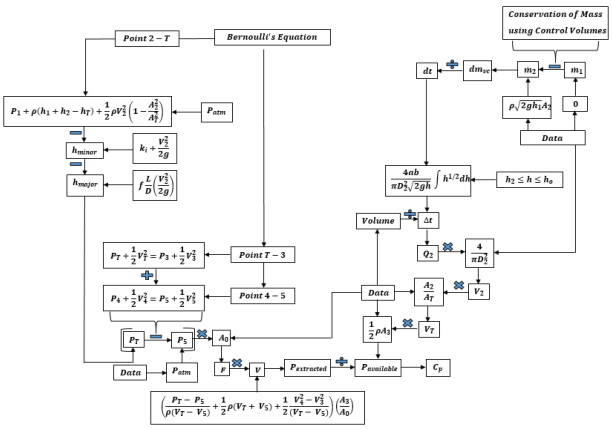

Fig. 2: Block Diagram of the Equations to Find the Boundary Conditions.

C. Modeling

Using ANSYS, 2D modeling is carried out for the resolution of the equations that govern the fluid dynamics. In this way, the pressure gradients in the wall are reached through the law of average speed. In addition, the turbulence is modeled on achievable k-epsilon. The SIMPLEC method of solution reduces the effect of the symmetry in two-dimensional mesh on the final solution, which allows to attach the pressure and speed with a correction of obliquity in one. Besides, a second order discretization was carried out: pressure, momentum, kinetic energy of turbulence ( ), dissipation of energy because of the turbulence ( ) [18].

The mesh of Fig. 3 presents characteristics such as: convergence of the simulation, smoothness, obliquity, aspect ratio, computational expense and margin of error, obtaining a triangular mesh, adaptable to the geometry of the turbine duct and with elements of good quality at 95.5%.

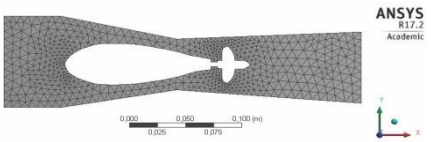

Fig. 3: Meshing Generated in Turbine Duct.

The boundary conditions were found taking into account the characteristics of the fluid (water) and the material (acrylic), which are: Density, specific heat, thermal conductivity and viscosity, as well as geographical aspects as the height of Quito at $2830msnm$ with an atmospheric pressure of 73923 Pa, ambient temperature of 15 $°C$, and the acceleration of gravity in 9.76 m/s^2.

III. RESULTS

Fig. 4 shows that from the maximum level to 1 m the height up to approximately 0.85 m, the water discharge in the turbine pipeline is sudden since the volume of earth on that interval is greater, increasing the magnitude of fluid velocity and thus greater speed of rotation in the axis of the permanent magnet generator, thus gaining greater removable power of approximately 2.022 W during that interval. It is also noted that, from the 0.85 m up to the height of 0.05 m, the power has a tendency almost linear as the level of the water is discharged, obtaining a minimum power of 0.032 W.

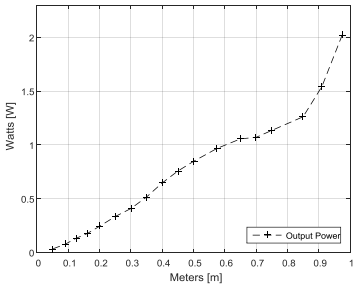

Fig. 4: The Electrical Power Generated in Pipeline vs Turbine Height of Water of the Reservoir.

Two variables that interfere in the interior of the duct of turbine for power generation (pressure and magnitude of speed) were identified and studied by means of analytical methods using domain limit parameters for the development of simulation, to be then compared with the data experimentally obtained using. Refer to (4), allowing to find the relative error of the simulated curve with respect to the experimental curve.

$$Error(\%) = \frac{\int_{0.15}^{1} |P_{CFD}(H) - P_{Experimental}(H)|}{\int_{0.15}^{1} |P_{CFD}(H)|} \quad (4)$$

Fig. 5 shows that the simulated curve compared with the experimental curve in pressure 1 (entry of the pipeline of turbine) maintains a linear trend. However, it is observed that the simulated curve presents no fluctuations in comparison with the experimental one. This is since the design between the area of the output section of the reservoir and the entry of the pipeline of turbine does not present a profile of entry of nozzle smoothed quarter circle, generating abrupt changes of load and speed in the flow, obtaining a relative error of 5.83 % between the curves.

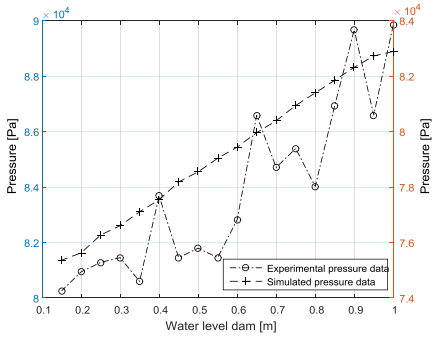

Fig. 5: Pressure 1 (Input to the Pipeline) vs Height of Water of the Reservoir.

Fig. 6 shows that the simulated curve compared with the experimental in pressure 2 (the end of the leeward side of the bulb) presents the same trend, however the simulated curve doesn't quite fit to the experimental one, this is because the pressure decreases as the level of reservoir water is discharged and the fluid velocity increases. In addition, there is a decrease in amplitude between ridges and valleys due to that the bulb presents less resistance to current flow for their hydrodynamic form resulting in softness in the losses for load, getting a relative error of 1.69% between the curves.

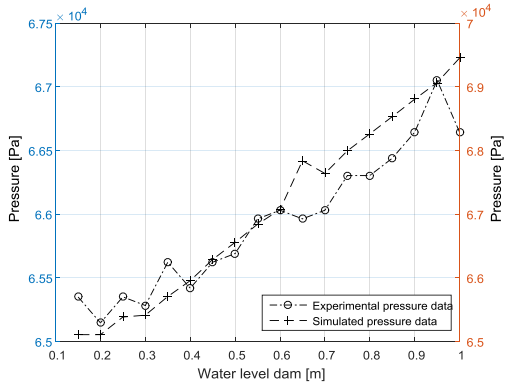

Fig. 6: Pressure 2 (End of the Leeward Side of the Bulb) vs Height of Water of the Reservoir.

Fig. 7 shows that the simulated curve compared with the experimental in pressure 3 (anterior to the propeller) shows the same trend. However, the experimental curve shows a linear behavior of almost , indicating that there is no turbulent fluid during all of the discharge at that point. Therefore, it is suitable to indicate, for the extraction of energy, that the pressure decreases, but it is greater at each point of pressure 2. This is due to the change of section converging to divergent from the geometry of the pipeline. Finally, it is noted that the simulation presents a pressure drop (increase in speed) to start the download indicating that the entry of water should be proportional to the opening of gates and not in a direct way. After this, the pressure is linear and agrees with the experimental data, thus obtaining a relative error 1.95% between the curves.

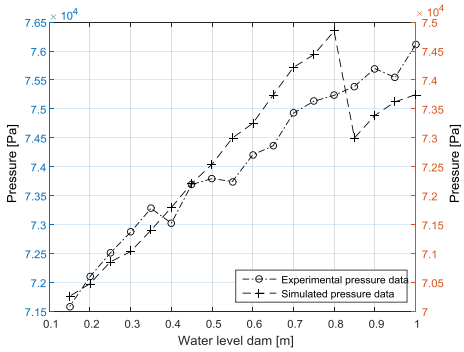

Fig. 7: Pressure 3 (Anterior to the Propeller) vs Height of Water of the Reservoir.

Fig. 8 shows that the two curves fluctuate and are with lower pressures on the front of the propeller during all the discharge points, indicating that the fluid velocity increases and is in turbulent mode. This is due to the fact that the propeller produces an additional propulsion thrust to the hydrodynamic force, generating an inertial force to the fluid, caused by the rotational movement of the blades, thus obtaining a relative error of 2.77% between the curves.

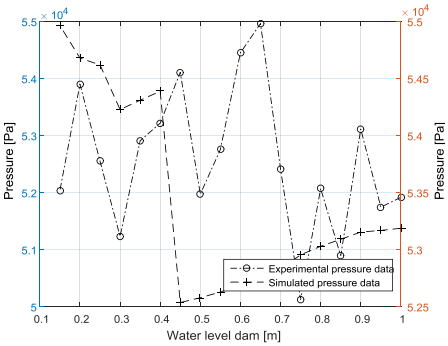

Fig. 8: Pressure 4 (Posterior to the Propeller) vs Height of Water of the Reservoir.

Fig. 9 (a) simulated, it is noted that the fluid presents a negligible kinetic turbulence from the head and end of the leeward to the anterior to the propeller. However, the behavior of the fluid in the back of the propeller presents the presence of turbulence in the kinetic energy of (k'') in the

instant of 900 ms after the opening of the gate of passage of water flow, in the same way as the experimental part, see Fig. 9 (b). It can be observed that there is no disturbance in the fluid until before the propeller, and after this, a bubble is generated in the form of reverse C at the instant of 850 s, thus obtaining a two-dimensional analysis predictive analytics in the interior of the turbine duct.

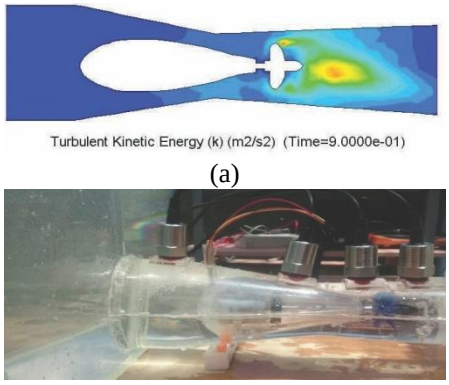

(a)

(b)

Fig. 1: Turbulent kinetic energy at the exit of the propeller simulated at 900 ms b) Appearance of bubble at the output of the propeller edited in video of 850 ms.

Fig. 10 shows that the fluid in the part simulated, compared with the experimental, remains undisturbed until the area in which is requires for power generation. It is also noted that, in both cases, the onset of turbulent kinetic energy after getting out from the propeller.

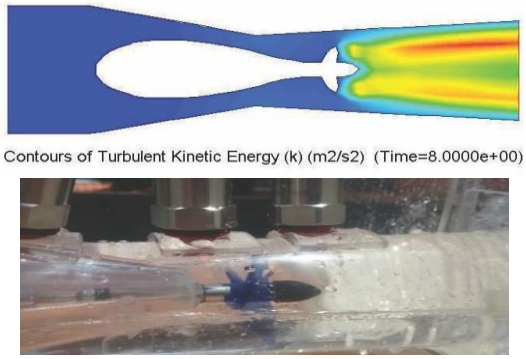

Fig. 10: Simulated turbulent kinetic energy and experimental in 8 seconds

IV. CONCLUSION

The experimental part and simulation showed that, during all the time it takes the water discharge, the turbulent kinetic energy presents a behavior of $k'' = 1.85x10^{-4}\, m^2/s^2$, this variable being negligible for the electric power generation. However, the data found in the CFD show that the turbulent kinetic energy becomes evident after the fluid passes out the propeller and it was observed in the experimental part.

With the results obtained in the 2D simulation and in experimental ones, it was observed that there is a qualitative and quantitative similarity in two inner points of the turbine pipeline called final part of leeward and anterior to the propeller. This is because the fluid is not disturbed by getting an error in those points of 1.69% and 1.95% respectively, validating the prediction. On the other hand, at the ends of the turbine pipeline called entrance of the pipeline and back of the turbine, it was noted that the simulation maintains a result of qualitative prediction in vortexes and cavitation. However, in the quantitative analysis, the two-dimensional simulation moves away from the experimental behavior getting an error of 5.83% and 2.77% respectively.

REFERENCES

1. Velasco, J. (2009). Energías renovables. Retrieved from. Available: https://books.google.com.mx/books?hl=es&lr=&id=bl6L8E_9t1kC&oi=fnd&pg=PA4&dq=energías+renovables&ots=r8kvhl-Me&sig=t0mlMjrTpcUFdiUONeC2kkdEqgY
2. IEA. (2017). Informing Energy Sector Transformations. Available: https://doi.org/10.1787/energy_tech-2014-en
3. REN21. (2017). Renewables 2017 Global Status Report. Avaible: https://doi.org/10.1016/j.rser.2016.09.082
4. Barnes, C. R., Best, M. M. R., Pautet, L., & Pirenne, B. (2011). Understanding earth- ocean processes using real-time data from NEPTUNE, Canada's widely distributed sensor networks, Northeast Pacific. Geoscience Canada, 38(1), 21–30.
5. Seyboth, K., Eickemeier, P., Matschoss, P., Hansen, G., Kadner, S., Scholomer, S., … von Stechow, C. (2011). Fuentes de energía renovables y mitigación del cambio climatico. Grupo Intergubernamental de Expertos sobre el Cambio Climático. Avaible: https://doi.org/ISBN 978-92-9169-331-3
6. Qin, C., & Chen Q (2015) 'A Coordinated Control Method to Smooth Short-Term Power Fluctuations of Hybrid Offshore Renewable Energy Conversion System (HORECS)', IEEE Eindhoven PowerTech, pp. 1–5.
7. Alonso, C., Gracia, F. J., Rodríguez-Polo, S., & Martín Puertas, C. (2015). El registro de eventos energéticos marinos en la bahía de cádiz durante épocas históricas. Cuaternario y Geomorfologia, 29(1–2), 95–117. Avaible: https://doi.org/10.17735/cyg.v29i1-2.29935
8. Alsina, S. B., & Castells, X. E. (2011). Energía, agua, medioambiente, territorialidad y sostenibilidad. Diaz de Santos, 25.
9. Creus, A. 2009. Energías renovables, (2a. ed.), Barcelona: Cano Pina.
10. Türkmen, S., Tağa, H., & Özgüler, E. (2013). Effect of Construction Material on Dam Type Selection of the Büyük Karaçay Dam (Hatay, Turkey). Geotechnical and Geological Engineering, 31(4), 1137–1149. Avaible: https://doi.org/10.1007/s10706-013-9640-8
11. Kothary, D. P., Signal, K. C., & Ranjan, R. (2011). Renewable energy sources and emerging technologies, 2a.ed, New Delhi, PHI Learning Private Limite.
12. Manzano, J., Palau, C. V., Benito, M. de A., Guilherme, V. do B., & Vasconcelos, D. V. (2016). Geometry and head loss in Venturi injectors through computational fluid dynamics. Engenharia Agrícola, 36(3), 482–491.
13. Ruiz, A., García, J., & Mesa, J. (2016). Error, incertidumbre, presición y exactitud, términos asociados a la calidad espacial de dato geográfico. Universidad de Jaén, 1-8.
14. Katam, V. (2005). Simulation of Low-Re Flow Over a Modified Naca 4415 Airfoil With Oscillating Camber, 159.
15. PropExpert. (2007). Definition of Propeller Tunnels for PropExpert, HydroComp Knowledge Library, 1.
16. Schneekluth, H., & Bertram, V. (2007). Ship propulsion. Ship Design for Efficiency and Economy, 180–205. Avaible: https://doi.org/10.1016/b978-075064133-3/50006-2

Published By:
Blue Eyes Intelligence Engineering
& Sciences Publication

17. Maldonado, F. (2005). Diseño de una turbina de río para la generación de electricidad en el distrito de Mazán-Región Loreto. Universidad Nacional Mayor de San MArcos, 69 Retrieved.Avaible: https://www.google.com.co/url?sa=t&rct=j&q=&esrc=s&source=web&cd=5&cad=rja&uact=8&ved=0ahUKEwiM5uSprs_SAhVW0WMKHRxqC8sQFggwMAQ&url=http%3A%2F%2Fsisbib.unmsm.edu.pe%2Fbibvirtualdata%2Fmonografias%2Fbasic%2Fmaldonado_qf%2Fmaldonado_qf.pdf&usg=AFQjCNHy9BX1tl
18. Gómez, G. C. (2012). Dinámica de Fluidos Computacional Dinámica de Fluidos Computacional.
19. Garcés, A. M., (2016). Diseño, Contrucció y Simulación del LLenado de un Molde en Arena en Verde para Fundición de Piezas de Aluminio Blanco. Escuela Politécnica Salesiana
20. Bergadà, J. M. 2012. Mecánica de fluidos: breve introducción teórica con problemas resueltos. Barcelona: Universitat Politècnica de Catalunya.
21. Çengel, Y. A., & Cimbala, J. M. (2006). Mecánica de fluidos: fundamentos y aplicaciones, Madrid: McGraw-Hill Interamericana.
22. Won, D. J., Kim, J., & Kim, J. (2015). Design optimization of duct-type AUVs using CFD analysis. Intelligent Service Robotics, 8(4), 233–245. Avaible: https://doi.org/10.1007/s11370-015-0179-9.
23. Kumar, D., & Sarkar, S. (2016). Numerical investigation of hydraulic load and stress induced in Savonius hydrokinetic turbine with the effects of augmentation techniques through fluid-structure interaction analysis. Energy, 116, 609–618. Avaible: https://doi.org/10.1016/j.energy.2016.10.012
24. White, F. M. 2004. Mecánica de fluidos, (5a. ed.), Madrid: McGraw-Hill España.

AUTHORS PROFILE

William Oñate obtained his Bachelor degree in Electronics and Control from Salesian Polytechnic University, Quito-Ecuador in 2014, and obtained a M.Sc. in Energy Efficient at National Polytechnic University, Quito-Ecuador in 2017. Currently he is a professor at the from Salesian Polytechnic University. His area of research is renewable energy controller system, intelligent control applied to improve process, artificial intelligence.

E-mail: wonate@ups.edu.ec
ORCID iD: 0000-0001-6982-2502

Santiago Maldonado received the Engineering degree in Electronics and Control from Universidad Politécnica Salesiana, Quito, Ecuador, in 2013, and obtained a M.Sc. in Industrial Automation and Control Systems in 2017 in Escuela Politécnica Nacional.

Sebastian Taco obtained his Bachelor degree in Chemical Engineering at Escuela Politécnica Nacional Quito-Ecuador in 2007. Then, he got his Master and PhD degrees in chemical engineering in Texas A&M University in 2009 and 2013, respectively. Dr. Taco has 4 publications, 2 books and 2 patents. Dr. Taco was a Fulbright scholar in 2007 and obtained the Brunner H. Barnes Scholarship Award in 2008.

Gustavo Caiza received the Engineering degree in Electronics and Control from Salesian Polytechnic University, Quito, Ecuador, in 2013, and obtained a M.Sc. in Industrial Automation and Control Systems in 2017. Currently he is a professor at the from Salesian Polytechnic University. His area of research is intelligent control applied to improve process, robotics, artificial intelligence and distributed control systems. He is a member of the IEEE.

E-mail: gcaiza@ups.edu.ec
ORCID iD: 0000-0002-8227-7227